

Stabilizing Motion Relative to an Unstable Orbit: Applications to Spacecraft Formation Flight

D. J. Scheeres,* F.-Y. Hsiao,[†] and N. X. Vinh[‡]

University of Michigan, Ann Arbor, Michigan 48109-2140

A control law is derived and analyzed that stabilizes a class of unstable periodic orbits in the Hill restricted three-body problem. The control law is derived by stabilizing the short-time dynamics of motion about a trajectory by the use of a feedback law specified by the instantaneous eigenvalue and eigenvector structure of the trajectory. This law naturally generalizes to a continuous control law along an orbit. By applying the control to an unstable periodic orbit, we can explicitly compute the stability of the control over long periods of time by computing the monodromy matrix of the periodic orbit with its neighborhood modified via the control law. For the case of an unstable halo periodic orbit in the Hill restricted three-body problem, we find that the entire periodic orbit can be stabilized. The resulting stable periodic orbits have three distinct oscillation modes in their center manifold. We discuss how this control can be applied to formation flight about a halo orbit. Some practical implementation issues of the control are also considered. We show that the control acceleration can be provided by a low-thrust engine and that the total fuel cost of the control can be quite reasonable.

I. Introduction

THIS paper studies the stabilization of an unstable periodic orbit in the Hill problem, which can serve as a general model for motion in the Earth–sun system. Results of this study will be relevant to the dynamics and control of a constellation of spacecraft in an unstable orbital environment such as found near the Earth–sun libration points. It will also shed light on the practical control and computation of a single spacecraft trajectory in an unstable orbital environment over long time spans.

We investigate the application of feedback control laws to stabilize a periodic orbit in the sense of Lyapunov (see Ref. 1) (note, not asymptotic stability). Thus, the stabilized trajectory will consist of oscillatory motions about the nominal trajectory, which in this context can be interpreted as motions in the center manifold of the stabilized periodic orbit. We show that an entire class of such control laws can be defined and their stability analyzed as a time-periodic linear system. The fuel expenditure for such control laws is often quite small and scales with the mean distance between the controlled motion and the nominal trajectory (which is a periodic orbit in this application). The problem of spacecraft control in unstable orbits is not new. (See Refs. 2 and 3 for reviews.) However, these previous studies have focused on stationkeeping control for a single spacecraft and have not considered how the relative motion of a formation of spacecraft could be stabilized and their dynamics modified, which is what we consider here.

Proposed space observatories of the future include ambitious interferometric imagers that use baselines of hundreds or thousands of kilometers between spacecraft to attain sufficiently high resolutions to image planets around distant stars. To carry out these imaging procedures requires that the relative motion between spacecraft be known extremely accurately and that the spacecraft “fill in” an effective image field as they move relative to each other. A periodic

halo orbit in the neighborhood of the Earth–sun L_2 libration point is an attractive region of space in which to fly such a formation of spacecraft, due to their consistent solar illumination characteristics, the lack of disturbing perturbations, and the relative ease of sending and retrieving spacecraft from this region. Specifically, it may be attractive to fly spacecraft formations about halo orbits in this region, flying the formation in the center manifold of a halo orbit, as was previously suggested by Barden and Howell.⁴ From a practical standpoint, however, the use of the center manifold of a natural halo orbit for constellation flight has two main drawbacks: The center manifold is itself unstable (because perturbations from the center manifold fall under the influence of the unstable manifold), and the rotation frequency of the center manifold is long, on the order of the halo orbit period (~ 6 months). Additionally, the “osculating plane” of the center manifold motion has a stringent orientation that cannot be modified. The current state of the art for computing and controlling spacecraft in the vicinity of a halo orbit can be found in Refs. 3–5. From these analyses, we see that extremely precise computations (numerical or analytical) are required to maintain an orbit in the center manifold of an unstable halo orbit because small deviations from the center manifold quickly cause the trajectory to diverge along the unstable manifold of the halo orbit.

In this paper, we propose an approach in the same spirit as the Barden and Howell⁴ work, but that addresses this problem from a different direction, casting the problem as a trajectory control problem from the start. Using this methodology, we change our focus from the computation of center manifold orbits to devising a simple control law that stabilizes the unstable periodic orbits and creates additional center manifolds within which a formation of spacecraft (or a single spacecraft) could be flown. Initially neglecting the issue of long-term stability, we first focus on stabilizing motion about an unstable orbit over short time spans. Technically, we wish to choose a control law that will establish Lyapunov stability of the relative motion. Having defined a control law that stabilizes relative motion over short time spans, we then generalize it to a control law over arbitrary time periods and apply it to an unstable halo orbit. We find that our approach yields a completely stable periodic orbit. The characteristics of the center manifolds of these stabilized periodic orbits can be changed by simply adjusting a single parameter in our control, yielding oscillation frequencies that can have an arbitrarily short period. Moreover, we show that the control law works in nonlinear situations as well and appears to be quite robust. Finally, we comment on the level of control acceleration needed and other practical issues of implementation, showing that the proposed control is quite reasonable.

Given the ability to stabilize a periodic orbit and choose the oscillation period of the resulting center manifolds, we can use such

Presented as Paper 2000-4135 at the AIAA/AAS Astrodynamics Specialist Meeting, Denver, CO, 14–17 August 2000; received 1 October 2001; revision received 10 July 2002; accepted for publication 24 July 2002. Copyright © 2002 by the authors. Published by the American Institute of Aeronautics and Astronautics, Inc., with permission. Copies of this paper may be made for personal or internal use, on condition that the copier pay the \$10.00 per-copy fee to the Copyright Clearance Center, Inc., 222 Rosewood Drive, Danvers, MA 01923; include the code 0731-5090/03 \$10.00 in correspondence with the CCC.

*Associate Professor of Aerospace Engineering, Department of Aerospace Engineering; scheeres@umich.edu. Senior Member AIAA.

[†]Graduate Student, Department of Aerospace Engineering.

[‡]Professor of Aerospace Engineering, Emeritus, Department of Aerospace Engineering.

a motion for application to the formation flight of spacecraft. In our proposed application, the control law would be used to generate relative motion between spacecraft in the formation, essentially causing them to wind around the periodic orbit, which we consider to be the nominal or mean path of the formation. For implementing this approach, a leader–follower system could be envisioned, with the leader spacecraft flying in the nominal periodic orbit and the follower spacecraft determining their position and, hence, creating a control law using relative measurements to the leader spacecraft. The relative motion between the spacecraft as they wind around the trajectory could then be used to cover an image plane and construct interferometric images of distant sources. Because the motion resulting from the current control law consists of three (linearly) separate center manifolds, we have considerable freedom to choose and change the relative motion throughout the orbit. Specifically, a variety of trajectories can be implemented by proper choice of the initial conditions and the application of one or two impulsive maneuvers can excite a different mode of the relative motion and change the dynamics of the constellation. Note that the approach and analysis of formation flight we are considering here differs from much of the previous work done in this area, which has focused on controlling spacecraft formations to stringent position and velocity constraints in a low-Earth-orbit (LEO) environment. In these other works, our approach is in spirit closest to the work reported by DeCou⁶ and Gómez et al.,⁷ where low-thrust propulsion is used to force a configuration of spacecraft to follow prescribed paths that can be used for interferometric imaging, and the work reported by Schaub et al.,⁸ Alfriend and Schaub,⁹ and Koon et al.,¹⁰ where they use the natural dynamics of the LEO environment to design formations that stay in close vicinity of each other without the introduction of control thrusts. In our application, we modify the local force structure using low-thrust engines to create a stable dynamic environment for the relative motion of the spacecraft.

II. Model of Motion

For computing the nonlinear motion, we use the Hill form of the three-body problem, which can be considered a simplified form of the three-body problem applicable to the motion of a spacecraft near the Earth and including the major perturbation term of the sun.¹¹ The three-dimensional motion is governed by the equations

$$\ddot{x} - 2\omega\dot{y} = \frac{\partial V}{\partial x} \quad (1)$$

$$\ddot{y} + 2\omega\dot{x} = \frac{\partial V}{\partial y} \quad (2)$$

$$\ddot{z} = \frac{\partial V}{\partial z} \quad (3)$$

$$V = \frac{\mu}{r} + \frac{1}{2}\omega^2[3x^2 - z^2] \quad (4)$$

where ω is the mean motion of the central, attracting body about the perturbing body (assuming circular motion) and μ is the gravitational attraction of the central body. In our situation, we choose μ to be that of Earth's and ω to correspond to an orbital period of one year. The x axis lies along the line from the perturbing body to the central body (the sun–Earth line) and remains fixed in this rotating frame. The y axis points along the direction of travel of the central body about the perturbing body, and the z axis is normal to the ecliptic. These equations are nonintegrable and exhibit a range of solutions analogous to solutions of the restricted three-body problem in the vicinity of the secondary. Note that these equations can be rescaled to remove all force parameters with the introduction of a scale length $(\mu/\omega^2)^{1/3}$ and a scale time $1/\omega$. In fact, this normalized form is the usual form in which the Hill problem is presented. In this paper, we retain dimensional values to stress the application to the Earth–sun system. (See Ref. 12 for a derivation of the Hill problem in the preceding form.) In the current work, we use the Hill problem because of its ease of specification, its applicability to motion in the vicinity of the Earth and sun, and its ability to be scaled to any of the planets and most of the planetary satellites. For applications to the Earth–sun system, the relative error introduced by use of the Hill

approximation, as compared to the restricted three-body problem, is on the order of 1.5%, meaning that results between the two systems usually differ by approximately this amount. This is also approximately equal to the order of magnitude of terms neglected when making the Hill approximation, or the mass of the Earth divided by the mass of the sun, raised to the one-third power.

For our investigation, we consider a periodic orbit solution of these equations: a halo orbit, to be more specific, which is a fully three-dimensional orbit centered about the libration points. Figure 1 shows this particular halo orbit projected into the main coordinate planes. The initial conditions of this periodic orbit are chosen to be similar to the Genesis halo orbit during its main mission phase.¹³ The period of this orbit is 178.9 days, and it is unstable with characteristic exponents $\sigma = \pm 4.757 \times 10^{-7}/s$ (a characteristic time of 24.3 days). The orbit also has a center manifold with two stable oscillation modes, one with a period equal to the periodic orbit (as all periodic orbits in time invariant systems have) and the other with a period slightly greater than one orbital period. This particular orbit was computed by numerical continuation from the family of Lyapunov orbits about the L_2 equilibrium point. The computation method we used is described in Ref. 14. Specifically, we first converged on a Lyapunov orbit of small amplitude using the linear solution for an initial guess. This family was then numerically continued by increasing the Jacobi constant in discrete increments (solving for the new periodic orbit at each point) until the critical bifurcation orbit was reached, where the halo orbits are born. The out-of-plane halo orbit family was then computed by starting from the critical orbit and inducing a small out-of-plane component. Once a member of the halo orbit was computed, this family was, in turn, continued numerically by increasing the Jacobi constant in increments until a halo orbit with similar amplitude characteristics to the Genesis trajectory was found. See the review by Howell¹⁵ for a more complete description of the halo orbits.

III. Relative Motion

For the development of our approach, we consider two trajectories in the Hill problem, one that follows the halo periodic orbit and a second trajectory in the vicinity of the orbit. For a leader–follower system, the leader spacecraft would be in the halo orbit, with the follower in its vicinity. The halo periodic orbit has a trajectory defined as $\mathbf{R}(t; \mathbf{R}_o, \mathbf{V}_o)$, $\mathbf{R}(t+T) = \mathbf{R}(t)$, where T is the period of motion. Naturally, the velocity of the motion, $\mathbf{V}(t; \mathbf{R}_o, \mathbf{V}_o)$, is also periodic with period T . The follower spacecraft has its own trajectory defined with position and velocity $\mathbf{r}(t; \mathbf{r}_o, \mathbf{v}_o)$ and $\mathbf{v}(t; \mathbf{r}_o, \mathbf{v}_o)$.

A. Linearized Dynamics

If the distance between the two solutions is relatively small, then the relative trajectory can be approximated using linearized equations of motion. Define $\mathbf{x} = [\mathbf{r}, \mathbf{v}]$, $\mathbf{X} = [\mathbf{R}, \mathbf{V}]$, and $\delta\mathbf{x} = \mathbf{x} - \mathbf{X}$, which is assumed to be “small” relative to the state \mathbf{X} . The dynamics of $\delta\mathbf{x}$ are

$$\delta\dot{\mathbf{x}} = \dot{\mathbf{x}} - \dot{\mathbf{X}} \quad (5)$$

$$\delta\dot{\mathbf{x}} = \mathbf{F}(\mathbf{X} + \delta\mathbf{x}) - \mathbf{F}(\mathbf{X}) \quad (6)$$

$$\delta\dot{\mathbf{x}} = \mathbf{F}(\mathbf{X}) + \frac{\partial \mathbf{F}}{\partial \mathbf{X}} \delta\mathbf{x} + \dots - \mathbf{F}(\mathbf{X}) \quad (7)$$

$$\delta\dot{\mathbf{x}} \sim \mathbf{A}(t)\delta\mathbf{x} \quad (8)$$

$$\mathbf{A}(t) = \frac{\partial \mathbf{F}}{\partial \mathbf{X}} \quad (9)$$

$$\mathbf{A}(t+T) = \mathbf{A}(t) \quad (10)$$

where $\mathbf{F}(\mathbf{X})$ is the dynamics function corresponding to Eqs. (1–3):

$$\mathbf{F}(\mathbf{X}) = \begin{bmatrix} \mathbf{V} \\ \frac{\partial V}{\partial \mathbf{R}} + 2\omega \mathbf{J} \cdot \mathbf{V} \end{bmatrix} \quad (11)$$

$$\mathbf{A}(t) = \begin{bmatrix} 0 & I \\ V_{RR} & 2\omega \mathbf{J} \end{bmatrix} \quad (12)$$

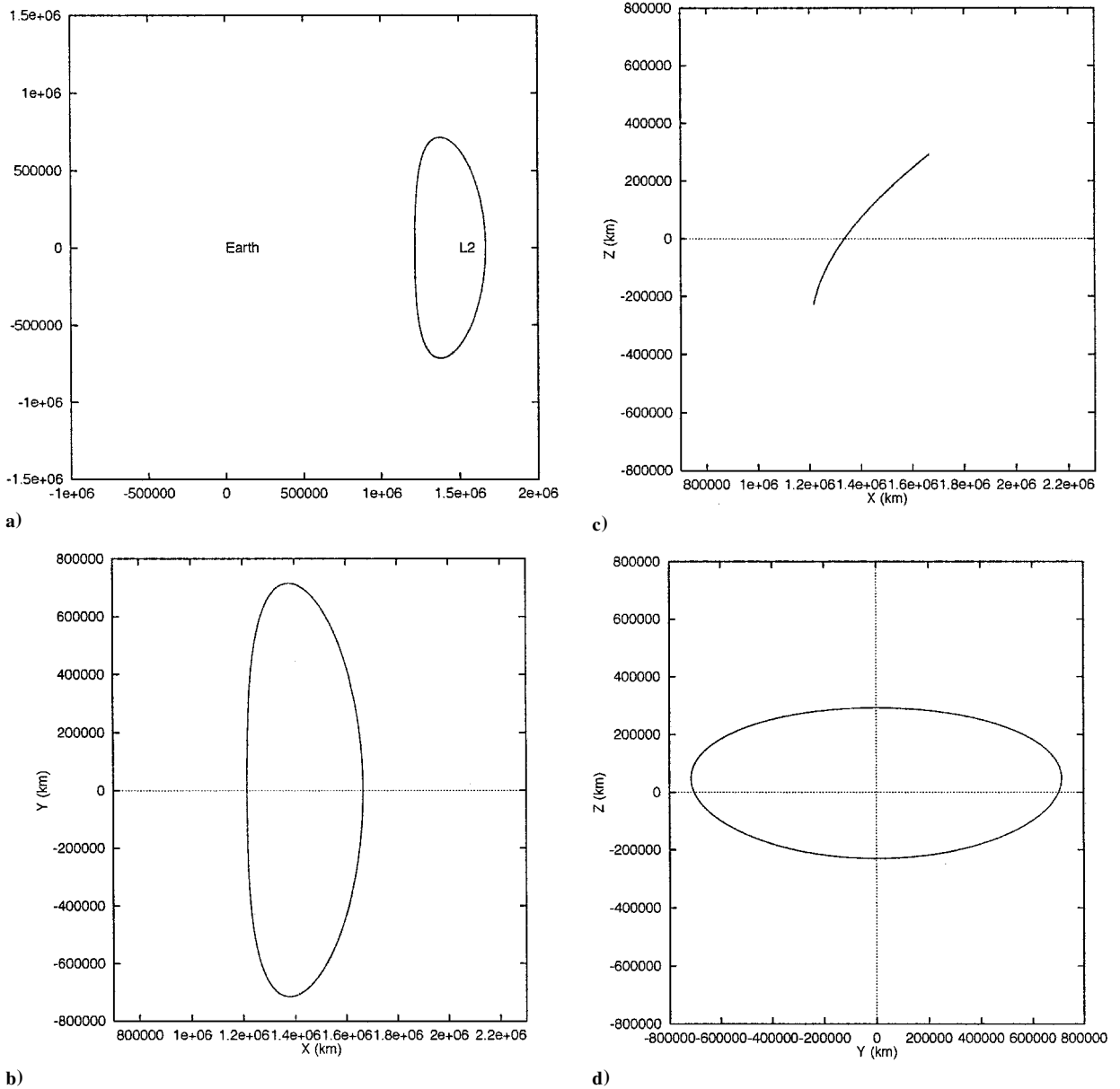


Fig. 1 Unstable halo periodic orbit: a) projection into the x - y plane, containing the attracting center; b) detail of x - y projection; c) projection of the halo orbit into the x - z plane; and d) projection of the halo orbit into the y - z plane.

$$J = \begin{bmatrix} 0 & 1 & 0 \\ -1 & 0 & 0 \\ 0 & 0 & 0 \end{bmatrix} \quad (13)$$

The solution for relative motion can then be expressed as

$$\delta \mathbf{x} = \Phi(t, t_o) \delta \mathbf{x}_o \quad (14)$$

$$\Phi(t, t_o) = \frac{\partial \mathbf{X}(t; \mathbf{X}_o)}{\partial \mathbf{X}_o} \quad (15)$$

$$\dot{\Phi}(t, t_o) = A(t) \Phi(t, t_o) \quad (16)$$

$$\Phi(t_o, t_o) = I \quad (17)$$

where Φ is the state transition matrix, computed about the periodic orbit, and $\delta \mathbf{x}_o$ is the initial offset of the follower spacecraft from the periodic orbit.

B. Long-Term Relative Motion

To analyze motion on the order of an orbit period or longer, it is customary to write the state transition matrix as the product of two

matrices by application of Floquet's theorem (see Ref. 16):

$$\Phi(t, t_o) = P(t - t_o) \exp(t - t_o) D \quad (18)$$

where P is a periodic matrix of period T and D is a constant matrix that has, as its eigenvalues, the characteristic exponents of the periodic orbit over one orbital period. As noted earlier in Sec. II, our periodic halo orbit has one pair of hyperbolic characteristic exponents and two circulation frequencies, one equal to the orbit period and one slightly longer. Because of the presence of the unstable manifold, uncontrolled relative motion will diverge from the vicinity of the periodic orbit with a time constant of ~ 23 days for our example orbit.

To maintain a long-term trajectory in the neighborhood of the periodic orbit, we must place it in the center manifold of the periodic orbit, defined as the space of orbits that do not lie along the hyperbolic manifolds of the periodic orbit. A spacecraft in such an orbit will naturally circulate about the periodic orbit in a quasi-periodic orbit, its trajectory winding onto a torus that encloses the periodic orbit in three-dimensional space.⁵ As discussed before, such a relative orbital configuration is attractive because, depending on the initial conditions given to the spacecraft, an ensemble of spacecraft distributed along such initial conditions may serve a useful

purpose as a constellation of spacecraft.⁴ However, as mentioned in the Introduction, the use of the natural center manifold is restrictive because it, too, is an unstable orbit and because it has a fixed oscillation frequency that is rather slow, with a period on the order of the orbit period.

C. Short-Term Relative Motion

For practical considerations, we may instead concern ourselves with the relative dynamics over a time much less than the orbital period. Although, in principle, the description of relative motion given in Eq. (18) holds true, it does not give us a direct indication of relative motion over shorter time periods.

We can represent the state transition matrix of the periodic orbit over one period as the product of mappings over much shorter time intervals within the period of motion:

$$\Phi(t_o + T, t_o) = \prod_{i=1}^N \Phi \left[t_o + \frac{T}{N}i, t_o + \frac{T}{N}(i-1) \right] \quad (19)$$

where the mapping over a time interval $\Delta t = T/N$ is represented as $\Phi(t_i + \Delta t, t_i)$ and conforms to the equation

$$\dot{\Phi}(t_i + \delta t, t_i) = A(t_i + \delta t)\Phi(t_i + \delta t, t_i) \quad (20)$$

$$0 \leq \delta t \leq \Delta t \ll T \quad (21)$$

For Δt small enough, we can expand $A(t)$ in a Taylor series expansion, yielding

$$A(t_i + \delta t) = A(t_i) + \dot{A}(t_i)\delta t + \dots \quad (22)$$

For our problem, we find that the force partial matrix $A(t)$ does not vary strongly over time, meaning that the time interval Δt can be chosen small enough to ensure that $\|A(t_i)\| \gg \|\dot{A}(t_i)\Delta t\|$. With this restriction, we find that the state transition matrix differential equation can be approximated over short time intervals as

$$\dot{\Phi}(t_i + \delta t, t_i) = A(t_i)\Phi(t_i + \delta t, t_i) + \dots \quad (23)$$

giving a time-invariant system at leading order. Thus, the solution can be expressed as

$$\Phi(t_i + \delta t, t_i) \sim \exp[A(t_i)\delta t] + \dots \quad (24)$$

$$\Phi(t_i + \delta t, t_i) \sim I + A(t_i)\delta t + \dots \quad (25)$$

where, because the time interval is chosen to be small, we neglect higher orders of the exponential expansion.

The relative motion can then be characterized over a short period of time by the eigenvalues and eigenvectors of the exponential map, defined from the equation

$$\Phi \mathbf{u} = \lambda \mathbf{u} \quad (26)$$

or, equivalently,

$$(\lambda I - \Phi)\mathbf{u} = 0 \quad (27)$$

where λ is the eigenvalue and \mathbf{u} is the eigenvector. With Eq. (25), this can be reduced to

$$\{[(\lambda - 1)/\delta t]I - A(t_i)\}\mathbf{u} = 0 \quad (28)$$

For a time-invariant system, the eigenvalue of the state transition matrix λ in Eq. (27) is equal to $e^{\gamma(\delta t)}$, where γ is the characteristic exponent of the system. Thus, the eigenvalue of Eq. (28) can be approximated as

$$\gamma \sim \lim_{\delta t \rightarrow 0} \frac{\lambda - 1}{\delta t} \quad (29)$$

From this sequence of approximations, we see that the relative motion of the spacecraft over a short time span centered at time t_i can be understood by analyzing the eigenvalues and eigenvectors of the matrix $A(t_i)$. Such an analysis resembles the analysis of an equilibrium point carried out at each time t_i . The errors induced by such an approximation are investigated in Ref. 17 and are shown to be reasonable.

Given the base periodic orbit, the characteristic exponents and frequencies of $A(t_i)$ can be computed at each point in time and are shown in Fig. 2. We see that, for our orbit, the structure is consistent, having a pair of hyperbolic roots and two pairs of oscillatory roots at each point along the orbit. In Appendix A, we discuss the regions in the Hill problem in which this structure exists and show that a large region around the libration points, enclosing our halo orbit, has this particular structure.

In deriving our control law, we will use these “short-term” dynamics to guide our thinking. It is a natural approach because one precursor for a spacecraft to diverge from a periodic orbit over a longer time span will be for it to diverge from the nominal trajectory over a shorter time span. Thus, we can think of relative motion along these “instantaneous” unstable manifolds to be a precursor to motion along the unstable manifold of the full orbit, as defined by Floquet theory. Note that the full orbit may still be unstable even if the instantaneous map is stable at each time step. We will see examples of this later.

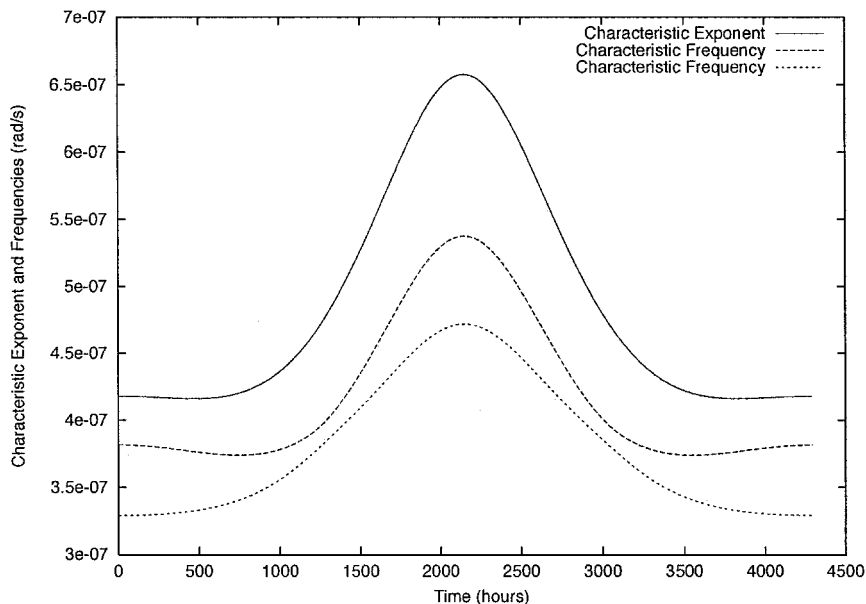


Fig. 2 Instantaneous characteristic exponents and frequencies of the periodic orbit over one period of motion.

IV. Stabilizing the Relative Motion

A control law is formulated that can stabilize the relative motion. We first derive the control by focusing on stabilizing the short-term dynamics, as described earlier. We then show that this “local stabilization” can also stabilize the long-term relative motion.

A. Local Stabilization

We propose a feedback control law that provides Lyapunov stability of our local, short time motion for a sufficiently large gain constant. To implement this control at a given time t_i , we evaluate the local eigenstructure of the matrix $A(t_i)$, find the characteristic exponents of the hyperbolic motion $\pm\sigma(t_i)$, and find the eigenvectors that define the stable and unstable manifolds of this motion $\mathbf{u}_{\pm}(t_i)$, where the plus denotes the unstable manifold and the minus denotes the stable manifold. To control the motion, we project the relative position vector (measured with respect to the periodic halo orbit at time t_i) into the stable and unstable manifolds, multiply by a gain constant, and apply a control acceleration along the stable and unstable manifolds, respectively. Thus, the control acceleration that we apply is

$$\mathcal{T}_c = -\sigma(t_i)^2 G [\mathbf{u}_+(t_i)\mathbf{u}_+(t_i)^T + \mathbf{u}_-(t_i)\mathbf{u}_-(t_i)^T] \delta \mathbf{r} \quad (30)$$

where G is the gain parameter and $\delta \mathbf{r}$ is the measured relative position vector, that is, the offset between the periodic orbit and the spacecraft at time t_i . We note that the eigenvalues $\pm\sigma(t)$ and eigenvectors $\mathbf{u}_{\pm}(t)$ are well-defined, periodic functions of time with period equal to the halo orbit period.

The linearized equations for relative motion are

$$\delta \mathbf{r}'' - 2\omega J \delta \mathbf{r}' - V_{rr} \delta \mathbf{r} = 0 \quad (31)$$

where ω is the rotation rate of the coordinate frame and $V_{rr}(t_i)$ is the second partial of the force potential [Eq. (4)] evaluated along the periodic orbit, making it a time-periodic matrix as well. Thus, the eigenvalues and eigenvectors that we use in our control scheme are computed from

$$[\sigma^2 I \mp 2\omega\sigma J - V_{rr}] \mathbf{u}_{\pm} = 0 \quad (32)$$

Implementing the control acceleration of Eq. (30) into Eq. (31) has the effect of modifying our potential force contributions to the linear system,

$$\delta \mathbf{r}'' - 2\omega J \delta \mathbf{r}' - \{V_{rr} - \sigma^2 G [\mathbf{u}_+\mathbf{u}_+^T + \mathbf{u}_-\mathbf{u}_-^T]\} \delta \mathbf{r} = 0 \quad (33)$$

This control law maintains the Lagrangian structure of the problem and provides local stability if the gain constant G is chosen sufficiently large. In Appendix B, we show that this control law can always stabilize a time-invariant, hyperbolic unstable two-degree-of-freedom system and give a heuristic justification for scaling our gain constant by the characteristic exponent squared. Note that an application of feedback control along the unstable manifold alone does not always stabilize the relative motion. This is also discussed in Appendix B.

The control law consists of a “reshaping” of the local force structure by proper application of thrusting. Because the magnitude of these forces is rather small in the vicinity of our halo orbit, the amount of acceleration needed to implement this control is also relatively small and could be provided by a low-thrust propulsion system in many cases.

B. Long-Term Stability

Equation (33) generalizes to relative motion over longer time spans as well because the eigenvalues and eigenvectors of the dynamic system are well defined as functions of time and because the structure of the local eigenvalues and eigenvectors does not change in the region around the halo orbit (see Appendix A). Thus, the stability of the resulting controlled orbit can be analyzed using classical techniques that have been developed for periodic orbits (c.f. Ref. 18).

1. Computation of Stability

Stabilization of the relative motion over short time spans does not necessarily guarantee that the motion of the spacecraft will be stable over longer time spans. Technical conditions for which such a time periodic system may be stable are discussed in greater detail in Ref. 16; however, even if these mathematical conditions are definite, they will not be easily applied to the current system, where we have fully general motion in three dimensions defined numerically and a linear map that changes significantly with time. The stability of the system can be evaluated, however, by application of Floquet theory and numerical integration.

The algorithm that we apply to evaluate stability is as follows. The periodic orbit and its accompanying state transition matrix, modified by introduction of the stabilization control, is numerically integrated over one period of motion. At each time step, the spectrum of the open-loop system is computed and fed into Eq. (33). The gain G is a constant free parameter that is specified at the start of the integration. The modified, time-varying matrix $\tilde{A}(t)$ used in the state transition matrix computation is

$$\tilde{A}(t) = \left[\begin{array}{c|c} 0 & I \\ \hline V_{rr}(t) - \sigma(t)^2 G [\mathbf{u}_+(t)\mathbf{u}_+(t)^T + \mathbf{u}_-(t)\mathbf{u}_-(t)^T] & 2\omega J \end{array} \right] \quad (34)$$

The resulting state transition matrix is denoted $\tilde{\Phi}(t_o + T, t_o)$, and the monodromy matrix evaluated over one period of motion is $\tilde{\Phi}(t_o + T, t_o)$. The minimum computation, then, consists of the integration of the periodic orbit (6 equations) plus the integration of the modified state transition matrix (36 equations). The integration was performed using a variable step size RK78 algorithm, with error control applied to the entire set of 42 equations. As the gain is increased, it is the numerical integration of $\tilde{\Phi}$ that controls the step size choice, and, hence, it is most convenient to carry along the computation of the periodic orbit because it and the spectrum of its local motion will then be evaluated at the appropriate time for inclusion in the $\tilde{\Phi}$ computation. This is found to be simpler than precomputing and storing the periodic orbit and its local stability characterization.

The stability of the closed-loop system can then be evaluated by computing the eigenvalues μ of this map (the monodromy matrix):

$$|\mu I - \tilde{\Phi}(t_o + T, t_o)| = 0 \quad (35)$$

As is well known, these eigenvalues must occur in complex conjugate pairs and in inverse pairs, meaning that for every eigenvalue μ , its complex conjugate $\bar{\mu}$ and its inverse μ^{-1} must also be eigenvalues. Stability of this system occurs when all of the eigenvalues have unit magnitude, that is, reside on the unit circle in the complex plane and, thus, have the form $\mu = e^{\pm i\theta}$. Conversely, an unstable map will either have a pair of multipliers along the real axis, of the form $\pm(\rho, 1/\rho)$, or will have a foursome of complex multipliers that lie off of the unit circle and have the form $\rho e^{\pm i\theta}, (1/\rho)e^{\pm i\theta}$. Either of these modes will lead to exponentially unstable relative motion.

2. Stability as a Function of Gain

As formulated, there is only one parameter for the controller, the gain constant G , and as this constant is increased, the stability characteristics of the monodromy matrix $\tilde{\Phi}(T)$ changes. For values of G when the monodromy matrix is stable, the space of all relative motions can be found by computing the characteristic frequencies and eigenvectors of the matrix. Motion under this map will, in general, lie on quasi-periodic tori surrounding the periodic orbit, similar to motion in the center manifold of a halo orbit, but with additional frequencies and elimination of instability concerns. Note that this control also eliminates the unity eigenvalues that give rise to “down-track” errors because the feedback control acts as a time-periodic forcing system that destroys the Jacobi integral, which, in turn, eliminates the unity eigenvalues. To give insight into the stability of this motion, we have evaluated the characteristics of the monodromy matrix for our orbit as G is increased. In Figs. 3 and 4 the Floquet multipliers are presented in the complex plane for varying values of

gain and their magnitudes are plotted as a function of gain, respectively. In Table 1, the stability of the system as a function of gain is summarized.

For $G < 1.17$, the control law has insufficient authority to stabilize the local motion at every instant along the periodic orbit, meaning that there are time intervals where the spectrum of $\tilde{A}(t)$ is not completely stable. We note that the monodromy matrix is also found to be unstable for this situation. Only for values of $G > 1.17$ is the instantaneous motion stable over the entire periodic orbit. However,

Table 1 Stability of the nominal halo orbit under the control

Gain	Stability	Description
< 1.17	No	Local dynamics not stable over the orbit
$1.17 < G < 2.19$	No	Local dynamics stabilized, but full orbit is not
$2.19 < G < 3.47$	Yes	First interval of stability
$3.47 < G < 5.21$	No	Single and double resonances with the orbit period
$5.21 < G < 5.92$	Yes	
$5.92 < G < 6.10$	No	Self-resonance between oscillation modes
$6.10 < G$	Yes	Except for small intervals of self-resonance

stability of the local motion does not guarantee stability of the monodromy matrix, and, in fact, we find that the monodromy map does not become stable until the gain G reaches a value of 2.19.

In general, the periodic orbit is stable for values of G greater than 2.19, but there are significant exceptions corresponding to resonances between the oscillation modes and resonances with the periodic orbit period. However, in analogy to the Mathieu equation, as the gain becomes larger, the size of these instability intervals become small. The first interval of instability occurs for $G \in [3.47, 5.21]$, which corresponds to single and double resonances with the orbital period and results in one pair of multipliers of the form $\rho_1, 1/\rho_1$ and another of the form $-\rho_2$ and $-1/\rho_2$ (visible in Fig. 3). The next interval of instability occurs for $G \in [5.92, 6.10]$, where two of the modes have a resonance, one having twice the period of the other, resulting in a complex set of four multipliers.

We note that the magnitude of the multipliers within these intervals of instability are “small,” the maximum multiplier in the aforementioned intervals being less than 1.1 over one orbit period (corresponding to a characteristic time greater than five years). This is especially small as compared to the original instability of the periodic orbit, which had a characteristic time of 23 days. In many cases, these instabilities would not appreciably hamper the use of this relative control. Moreover, such intervals of instability are expected and, in general, correspond to the eigenvalues of the monodromy map intersecting on the unit circle. As noted in Ref. 18, the presence of complex eigenvalues on the unit circle does not imply nonlinear stability of the relative orbits, but it does assure us that any nonlinear instabilities will not grow exponentially in time, but will only grow, at most, as a polynomial in time. For practical considerations, this implies that such instabilities should be controllable by standard navigation practices.

Note that for this stabilization control to work on our halo orbit, both the unstable and stable manifolds must be present in the feedback loop. A feedback loop that only cancels the local unstable manifold does not stabilize the orbit for any value of gain.

3. Characteristics of the Center Manifolds

Note that the stability structure of our stabilized periodic orbit is different than is usually found for time-invariant systems. Generally, every periodic orbit in a time-invariant system has an oscillation mode with period equal to the periodic orbit, leading to a pair of unity eigenvalues. This can be directly related to the existence of the Jacobi integral for time-invariant Lagrangian systems. In our controlled system, these unity eigenvalues do not exist, however, because the feedback control essentially changes the force structure of the system, creating a time-periodic system. Such systems do not have a Jacobi integral, and, thus, our stabilized periodic orbit has no eigenvalues identically equal to unity.

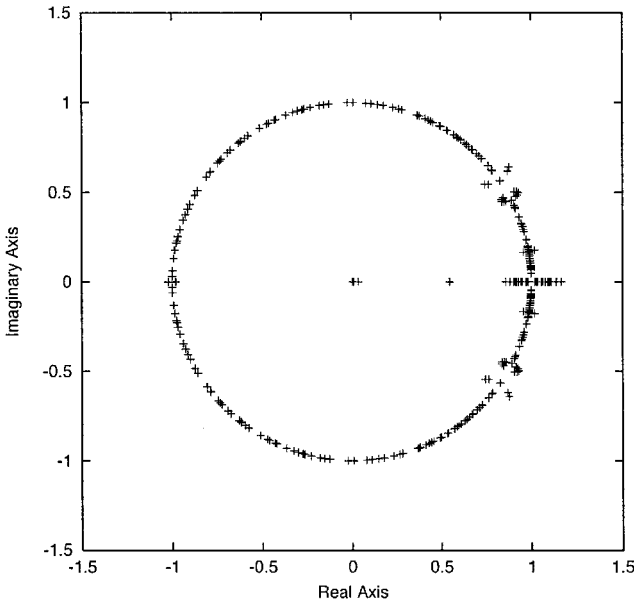


Fig. 3 Floquet multipliers of the controlled periodic orbit plotted on the complex plane.

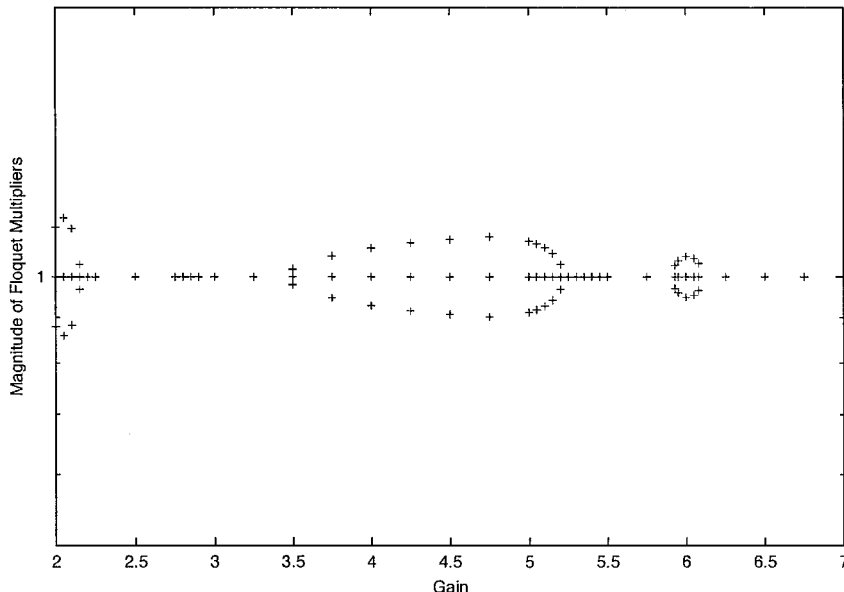


Fig. 4 Magnitude of the Floquet multipliers of the controlled periodic orbit as a function of the gain; for $G < 2.19$, there are always some multipliers not equal to one.

Thus, for the case of a completely stable monodromy matrix, there are three pairs of eigenvalues, each pair characterized by an angle θ_i , $i = 1, 2, 3$, measured on the unit circle.¹⁸ This angle denotes the total winding angle of the mode about the periodic orbit, modulus 2π . Taken together, they define a quasi-periodic orbit with three separate “average” periods over one halo orbit period. For the general characterization of these oscillation modes, we can consider the angles to be functions of time along the orbit $\theta_i(t)$, with their final values computed from the monodromy map being $\theta_i = \text{mod}[\theta_i(T), 2\pi]$. Unfortunately, there is no direct way to extract $\theta_i(t)$ from the numerically computed monodromy map. (See Gómez and Mondelo⁵ for a discussion of how these angles can be computed numerically.) This is an item of interest, however, because the frequency of these stable motions will change with the gain constant G and can be much larger than the periodic orbit frequency, meaning that a spacecraft having motion along one of these modes can encircle the periodic orbit many times over one period. Thus, defining and computing these mean frequencies is of practical interest for the relative motion. Ideally, we can compute these oscillation frequencies as

$$\bar{\omega}_i = \theta_i(T)/T \quad (36)$$

$$\bar{\omega}_i = 2\pi N_i + \theta_i \quad (37)$$

We find that the winding number N_i can be estimated from the time history of the spectrum of the state transition matrix $\tilde{\Phi}$ by counting the positive real axis crossings of the stable modes; however, this approach is not always well-defined because the intermediate spectrum of the matrix is not always stable. A different approach to this computation that works when the numbers N_i become relatively large is to estimate the angle $\theta_i(t)$ by performing the quadrature

$$\tilde{\theta}_i(t) = \int_0^t \tilde{\omega}_i(t) dt \quad (38)$$

where the frequency $\tilde{\omega}_i(t)$ is defined as an instantaneous characteristic frequency of the linear matrix $\tilde{A}(t)$, which has been stabilized by application of our control law. We find that reasonable estimates of the mean frequency of the stable modes of the relative motion can be found from this quadrature. Improvements to this approach will be investigated in the future.

As the gain of the control loop increases, the mean oscillation frequencies of the system $\bar{\omega}_i$ change, as noted earlier. For our system, one of these mean frequencies remains relatively constant and is consistently less than the periodic orbit frequency ($2\pi/T$). This oscillation mode is associated most strongly with “out-of-plane” motion along the z axis of the system and is related to the initial stable oscillation mode of the uncontrolled relative motion. Although the control loop does influence this stable oscillation mode, it never causes it to stray far from its original value.

Conversely, the mean frequency of the other two oscillation modes increase, in general, as the square root of the gain G . One of these modes originates from the original open-loop oscillation of period T , whereas the other is created when the closed-loop control removes the hyperbolic manifolds. By specification of the control gain G , the dynamics of the relative motion can be changed. For large values of G , these mean frequencies are approximately equal to $\sigma\sqrt{G}$ and $\sigma\sqrt{G}/2$, where $\sigma \sim 4.7 \times 10^{-7}/s$ is the characteristic exponent of the open-loop unstable periodic orbit. In terms of oscillation period for the relative motion, these are approximately $154/\sqrt{G}$ days and $309/\sqrt{G}$ days for our orbit (assuming $G \gg 1$).

A second item of interest is the orientation of these center manifold orbits in space. An approximate description of these can be evaluated by computing the eigenvectors of the controlled instantaneous linear map $\tilde{A}(t)$ defined in Eq. (34). The error associated with this approximation has been shown to be reasonable¹⁷ and provides an explicit computation of the osculating orbit plane that motion on the center manifold will follow. Figure 5 shows the linearized motion corresponding to the two fast center manifolds relative to the halo orbit over one halo orbit period. These osculating linear ellipses are plotted every 10 days and correspond to a gain $G = 10$. The period of motion on these ellipses is on the order of 50 and 100 days, respectively. Figure 6 shows the inclination and node of

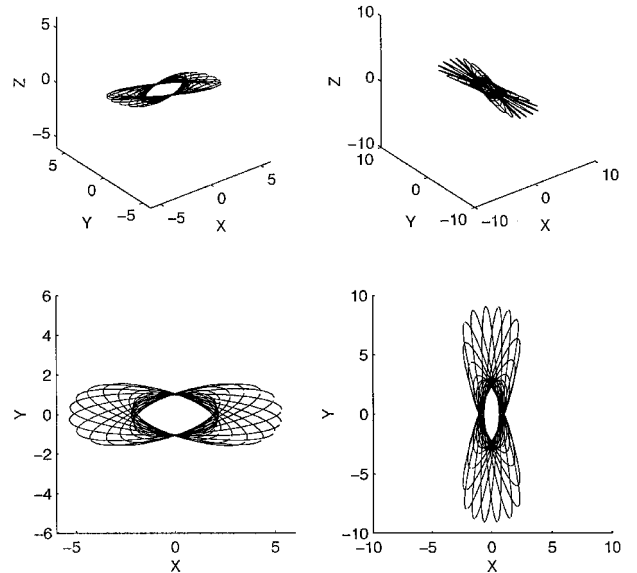
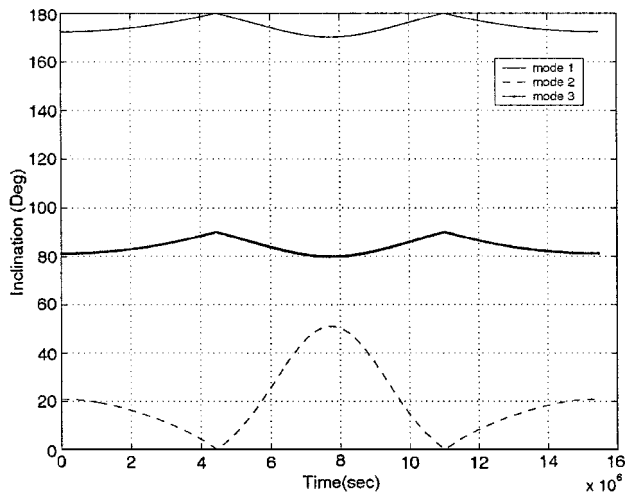
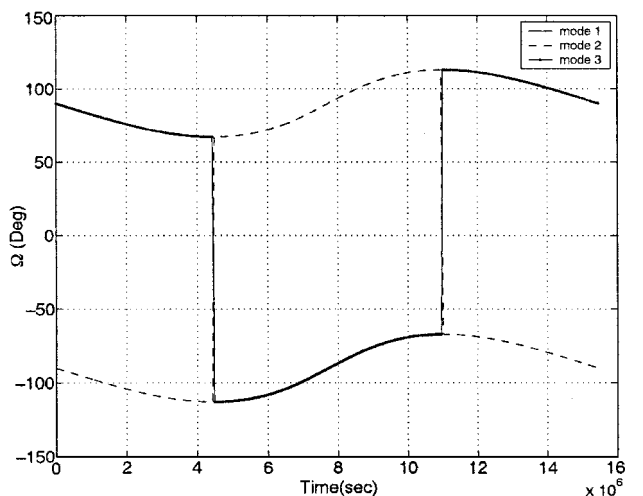


Fig. 5 Plots of the two high-frequency osculating linear ellipses in the center manifold about a stabilized periodic orbit; the ellipses are shown relative to a moving point on the halo orbit in the Earth-sun fixed frame of the Hill problem and are plotted every 10 days over the orbit period.

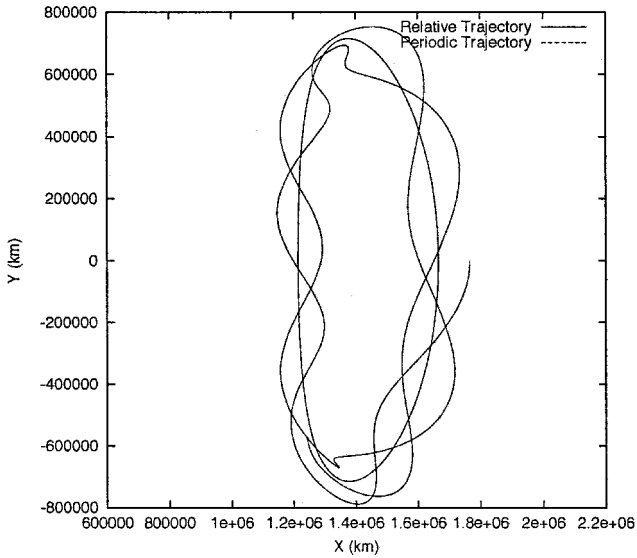


a)

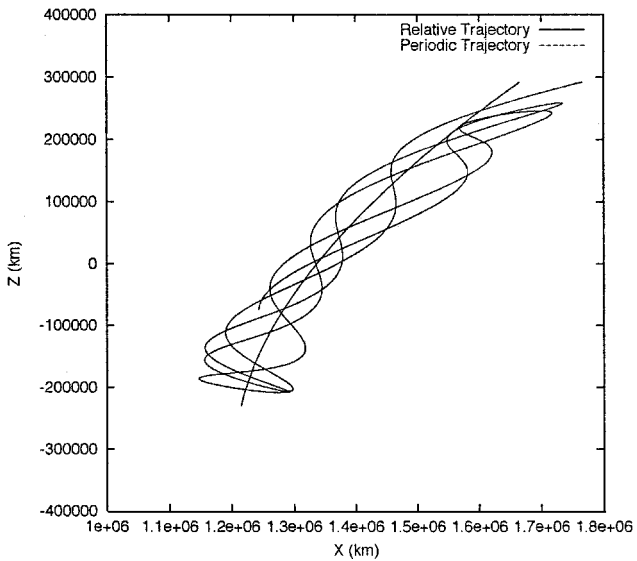


b)

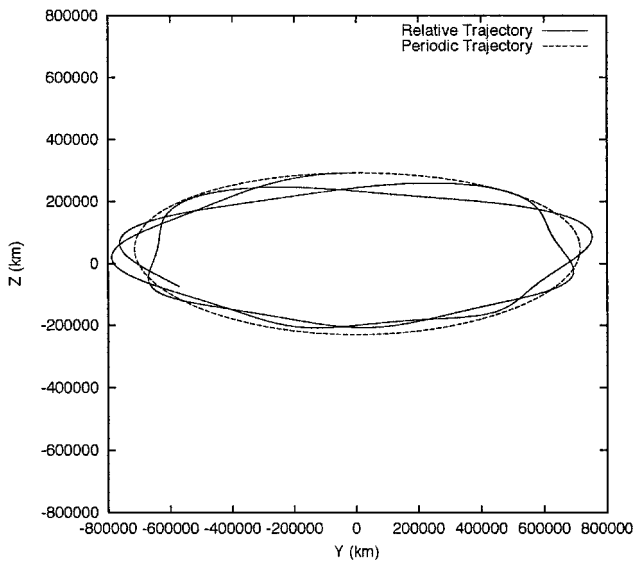
Fig. 6 Plots showing the plane orientation of the osculating linear ellipses of the center manifold over one halo period relative to the rotating Earth-sun frame: a) inclination of the orbit planes and b) node angle of the orbit planes.



a)

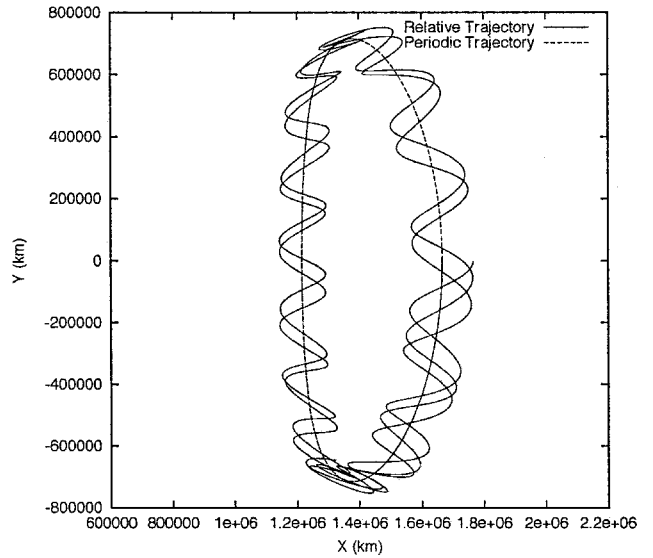


b)

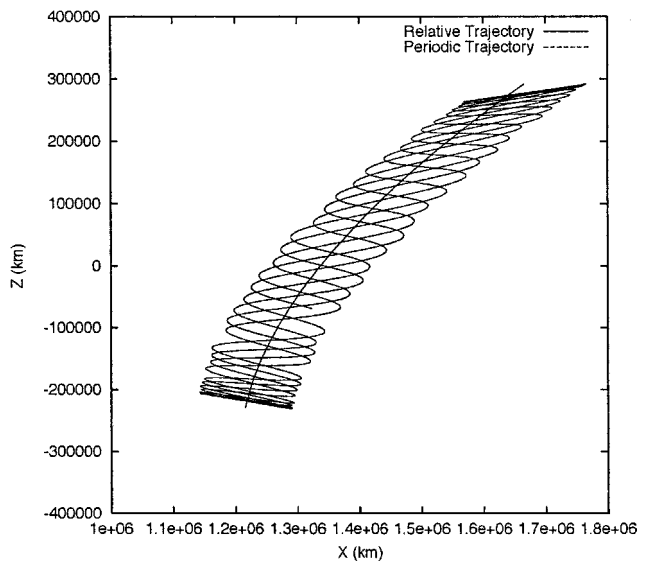


c)

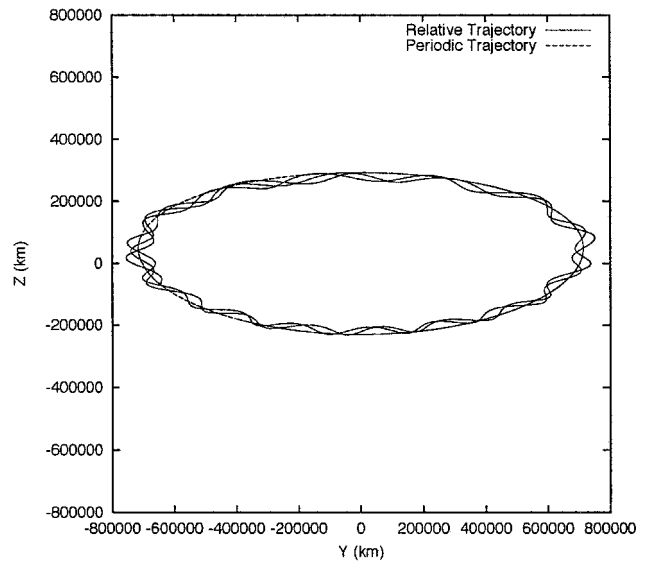
Fig. 7 Controlled trajectory and halo orbit projected into a) x - y plane, b) x - z plane, and c) y - z plane; control gain of 10 is applied with an initial position offset of 1×10^5 km.



a)



b)



c)

Fig. 8 Controlled trajectory and halo orbit projected into a) x - y plane, b) x - z plane, and c) y - z plane; control gain of 100 is applied with an initial position offset of 1×10^5 km.

these linear solutions for each of the center manifold model (relative to the rotating Earth–sun line).

4. Stability of Nonlinear Motion

Now that the linear stability of the control law for our halo orbit has been established numerically, it is of interest to verify that it can stabilize a nonlinear trajectory about a periodic orbit. To verify this, we apply the control acceleration given in Eq. (30) to the full equations of motion of a spacecraft in Eqs. (1–3). The initial conditions of this motion are denoted as an offset from the initial conditions of the periodic orbit at the initial time, and the relative position between the trajectory and the periodic orbit, needed for the control, is computed as the vector difference between the two solutions at each moment in time. This formulation is entirely consistent because the computed difference is equivalent to the measured relative difference, and the local stability computations are based on the periodic orbit, which can, in principle, be computed onboard the controlled spacecraft.

To push the control law to a somewhat extreme condition, we gave the spacecraft an initial position offset from the periodic orbit of 1×10^5 km with gains of 10 and 100. The resulting trajectories are

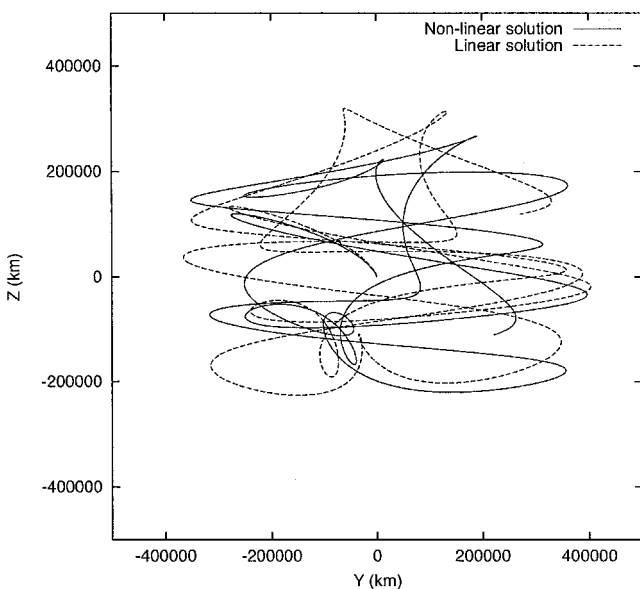


Fig. 9 Nonlinear and linear trajectory computations relative to the periodic orbit, projected into the y - z plane; control gain of 10 is applied, with an initial position offset of 5×10^5 km.

shown in Figs. 7 and 8. Each of these trajectories is integrated over 400 days, which is more than two periods of the periodic orbit. We note that our control law is able to maintain the stable relative motion over this time frame. Note that the computation of the periodic orbit itself over this length of time is nontrivial, due to the strength of its instability.

We also note that the control law is being applied in a region where nonlinearities dominate the system. In Fig. 9, we show a plot of the motion relative to the periodic orbit for a case with an initial position offset of 5×10^5 km and control gain of 10, projected into the y and z coordinate planes. Also shown is the linear solution to Eq. (33), started with the same value of offset, but obviously following a different trajectory as compared to motion in the “real” system. This gives an indication that our control law remains robust when the relative motion can no longer be approximated by the linear equations of motion.

V. Implementation

Now that we have shown that our control law stabilizes the periodic orbit and is robust when applied to fully nonlinear motion, it is necessary to compute the thrust needed to apply the control properly. The scenario we propose here consists of a spacecraft flying in a stabilized trajectory about a nominal periodic orbit. We only concentrate on the control of the relative motion. In our computations, we keep track of the total ΔV expended by performing the quadrature

$$\Delta V(t) = \int_0^t |\mathcal{T}_c| dt \quad (39)$$

The actual time history of the instantaneous thrust and accumulated ΔV changes as the gain and initial conditions are varied. Figure 10 shows the computed time histories for the control accelerations. An estimate of the necessary thrust level at any instant can be given by the relation

$$T_c \sim 2\sigma^2 GR \quad (40)$$

where R is the amplitude of the relative motion of the spacecraft, $\sigma \sim 4.7 \times 10^{-7}/s$ is the characteristic exponent of our periodic orbit, and G is the control gain. Thus, the thrust will scale as $0.44GR$ nm/s².

To apply a gain of 100 (oscillation periods of 15 and 31 days), with a relative constellation size of 1000 km, requires an acceleration of $44 \mu\text{m/s}^2$. For a 1000-kg spacecraft, this translates into a thrust of 44 mN. For a low-thrust ion engine with a characteristic velocity of 30 km/s over a 1-year mission, the resulting mass fuel fraction used is less than 5%.

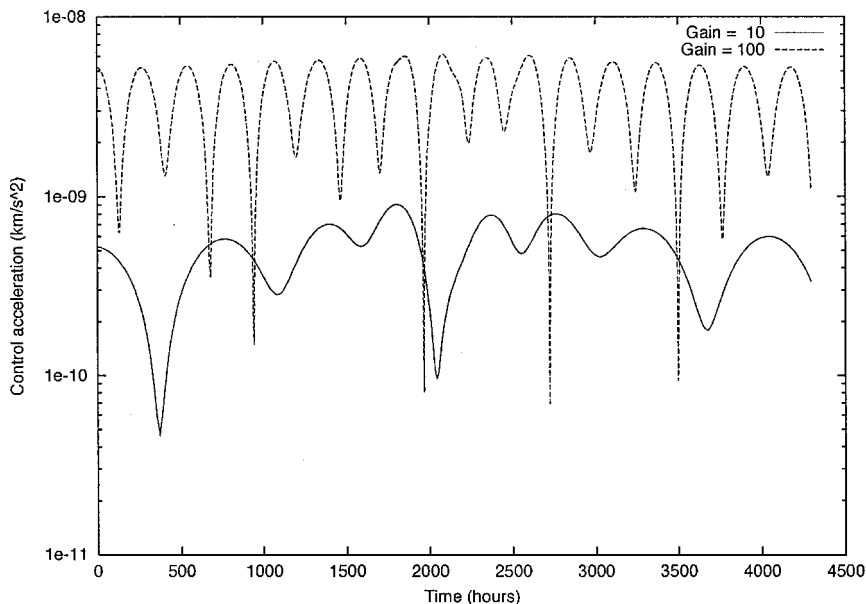


Fig. 10 Control acceleration time history for two trajectories, each with an initial offset of 700 km.

In the context of our proposed application, a “central” spacecraft might be in orbit along the unstable halo orbit, with its trajectory controlled using traditional navigation methods (or perhaps using our proposed control). The formation would then consist of spacecraft in neighboring orbits, each using the proposed control law to modify their motion relative to the central spacecraft. To successfully apply the control law, the position of each spacecraft must be measured relative to the central spacecraft. The radial distance and radial rate can be measured with a ranger and Doppler extractor. (We assume near-continuous communication between the spacecraft in support of their scientific mission.) If multiple receivers are placed on the spacecraft, the relative orientation of the spacecraft can be determined, and, by processing the inertially measured attitude, the relative position of the spacecraft can be determined at each moment. Additionally, the instantaneous unstable and stable manifolds of the central spacecraft can be easily computed, yielding all of the necessary information to compute and apply the feedback control law. In Ref. 19, it was found that the orbit uncertainty of a single spacecraft in an unstable halo orbit tended to be minimized along the local stable and unstable manifolds of the trajectory. A similar result for the relative orbit determination between two spacecraft would support the potential feasibility of our proposed approach to trajectory control.

VI. Conclusions

This paper analyzes the control of relative motion about an unstable periodic halo orbit about an Earth–sun libration point. A feedback control law is proposed that can stabilize this relative motion, creating a six-dimensional center manifold within which a spacecraft (or a formation of spacecraft) can orbit. The oscillation period of the controlled trajectory about the nominal orbit can be controlled by adjusting a single gain, generating relative motion that winds around the orbit many times over one halo orbit period. The control law is based on computing the “local stability” characteristics of the nominal motion and extends naturally to general trajectories. We show that the fuel costs of the control are reasonable and that the control could be implemented using a low-thrust propulsion device.

Appendix A: Region of Validity in the Hill Problem

The controller is only defined for systems whose instantaneous dynamics matrices $A(t)$ have a particular structure, one pair of real eigenvalues and two pairs of imaginary eigenvalues. Given the form of A

$$A = \begin{bmatrix} 0 & I \\ V_{rr} & 2\omega J \end{bmatrix}$$

we can show that its eigenvalue equation has the form

$$|\lambda I_{6 \times 6} - A| = |\lambda^2 I_{3 \times 3} - 2\omega\lambda J - V_{rr}|$$

which can be expanded as

$$\lambda^6 + b\lambda^4 + c\lambda^2 + d = 0 \quad (\text{A1})$$

By changing the variable to $\Lambda = \lambda^2$, we find a simple cubic equation:

$$\Lambda^3 + b\Lambda^2 + c\Lambda + d = 0 \quad (\text{A2})$$

For our control to be defined, this polynomial must have one positive and two negative roots. To find conditions on the polynomial coefficients, we use two results from the theory of equations. First, for all of the roots to be real and distinct, the discriminant of the equation Δ must be greater than zero²⁰:

$$\Delta = b^2c^2 + 18bcd - 4c^3 - 27d^2 - 4b^3d > 0 \quad (\text{A3})$$

Second, to investigate the signs of roots we use the Descartes rule of signs:

The number of positive roots of an equation with real coefficients either equals the number S of variations of signs in the series of coefficients or is less than S by an even integer.

To apply these results, we must evaluate the coefficients in our cubic polynomial. First, we compute V_{rr} , the second derivative of

potential energy with respect to r . Before performing this computation, we take advantage of the special structure that the Hill equations have and rescale them to remove all parameters, yielding

$$V = 1/r + \frac{1}{2}(3x^2 - z^2) \quad (\text{A4})$$

$$V_{rr} = -(1/r^3)I + (3/r^5)rr + 3\hat{x}\hat{x} - \hat{z}\hat{z} \quad (\text{A5})$$

Carrying out the computations yields the coefficients of Eq. (A2),

$$b = 4 - (v_{xx} + v_{yy} + v_{zz}) = 2 \quad (\text{A6})$$

$$c = v_{xx}v_{yy} + v_{yy}v_{zz} + v_{xx}v_{zz} - v_{xy}^2 - v_{yz}^2 - v_{xz}^2 - 4v_{zz} \quad (\text{A7})$$

$$d = -|V_{rr}| \quad (\text{A8})$$

where v_{ij} , $i, j = x, y, z$, are the elements of matrix $[V_{rr}]$.

When the Descartes rule of signs is followed, because $b > 0$, our conditions for one change of sign are satisfied if $d < 0$, that is, the determinant of V_{rr} must be greater than zero. Thus, we must determine regions where both $|V_{rr}| > 0$ and $\Delta > 0$ are satisfied. We first consider the condition $|V_{rr}| > 0$. In particular, we look at this condition in the planes $z = 0$, $y = 0$, and $x = 0$.

For the XY plane, set $z = 0$, then $r^2 = x^2 + y^2$, $x/r = \cos\theta$, and $y/r = \sin\theta$. Then we find that the condition $|V_{rr}| > 0$ reduces to

$$-2 - 3r^3 + 9r^3 \sin^2\theta < 0 \quad (\text{A9})$$

or

$$r^3 < 2/(9 \sin^2\theta - 3) \quad (\text{A10})$$

$$\sin^2\theta < (2 + 3r^3)/9r^3 \quad (\text{A11})$$

When $\theta = \pm 90$ deg, $|y| = r < 0.69$. When $r \rightarrow \infty$, the boundaries lie along the asymptotes with $\theta = \pm 35.26$ and ± 144.74 deg. See Fig. A1a for a plot of these regions.

For the XZ plane, set $y = 0$, then $r^2 = x^2 + z^2$, $x/r = \cos\theta$, and $z/r = \sin\theta$. Then the condition $|V_{rr}| > 0$ reduces to

$$-3r^6 + (12 \sin^2\theta - 5)r^3 - 2 < 0 \quad (\text{A12})$$

When $\theta = \pm 90$ deg, $|y| = r > 1.26$ or $|y| = r < 0.69$. When $-65.26 < \theta < 65.26$ deg, or $114.74 < \theta < 245.26$ deg, the condition is valid everywhere. See Fig. A1b for a plot of these regions.

For the YZ plane, set $x = 0$, then $r^2 = y^2 + z^2$, $y/r = \cos\theta$, and $z/r = \sin\theta$. Then the condition $|V_{rr}| > 0$ reduces to

$$(-2 + r^3 - 3r^3 \cos^2\theta)[-(1/r^3) + 3] > 0 \quad (\text{A13})$$

or

$$\begin{cases} r < 0.69, & -2\pi < \theta < 2\pi \\ \theta = \pm 90 \text{ deg}, & |y| = r > 1.26 \\ r \rightarrow \infty, & \begin{cases} 122.26 > \theta > 57.74 \text{ deg} \\ -122.26 < \theta < -57.74 \text{ deg} \end{cases} \end{cases} \quad (\text{A14})$$

See Fig. A1c for a plot of these regions.

In our specific problem, we are interested in applying the control to a trajectory in the vicinity of the libration points in the Hill problem. Thus, in Fig. A1d, we also show a cross section of the YZ plane at the value $x = (1/3)^{(1/3)} \sim 0.69$, which is the equilibrium point location in the normalized Hill problem. We note that the orbit we are interested in is clearly contained within the applicable region.

For the constraint on discriminant Δ , $\Delta > 0$ was evaluated numerically and found to be satisfied whenever $|V_{rr}| > 0$ was satisfied. Thus, the controlling condition on our system is $|V_{rr}| > 0$, and an analytical discussion of the regions where $\Delta > 0$ is not needed.

From our discussion, we see that our control law is valid around the libration points in the Hill problem. In terms of our physical problem, we see that the valid area for our control is defined by the determinant of the V_{rr} matrix being positive.

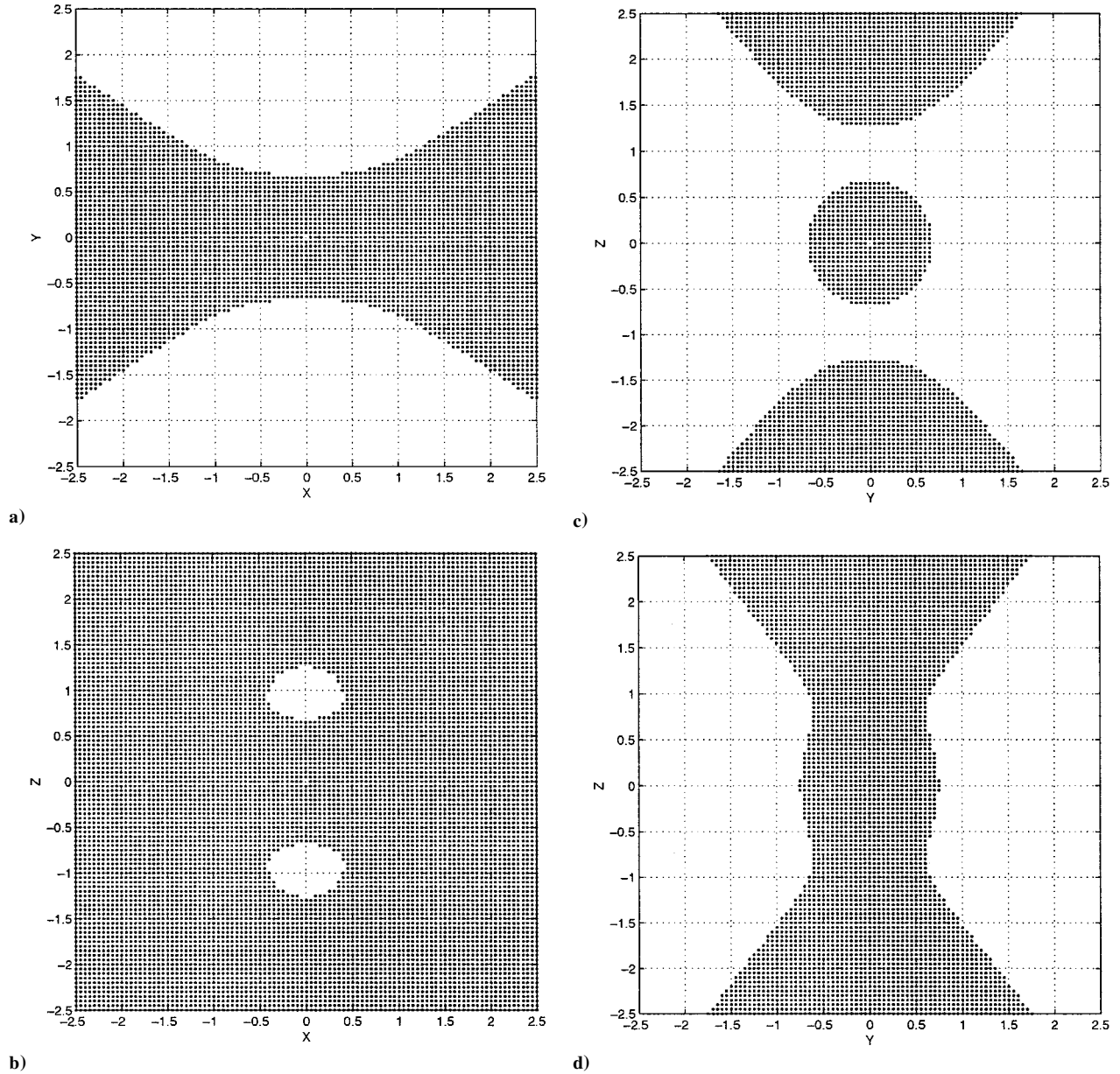


Fig. A1 Regions where $|V_m| > 0$ projected into a) x - y plane with $z = 0$, b) x - z plane with $y = 0$, c) y - z plane with $x = 0$, and d) y - z plane with $x = (1/3)^{1/3}$; libration points are located at $x = \pm(1/3)^{1/3} \sim \pm 0.69$.

Appendix B: Stabilization of Hyperbolic Unstable Systems

We first consider stabilization of a simple, one-degree-of-freedom hyperbolic unstable motion. The generic form for this case is

$$\ddot{r} - \sigma^2 r = 0 \quad (\text{B1})$$

where σ is the characteristic exponent of the unstable system. In this case, an intuitively obvious stabilization is to apply a position feedback acceleration of the form $-Kr$, yielding the modified system

$$\ddot{r} - (\sigma^2 - K)r = 0 \quad (\text{B2})$$

Then the condition for Lyapunov stability is $K > \sigma^2$, or, rewriting as $K = \sigma^2 G$, the stability condition becomes $G > 1$. This simple result motivates us to scale our feedback gain by the square of the local characteristic exponent.

Next, consider the application of our control scheme to an unstable hyperbolic point in a rotating two-degree-of-freedom frame. The open-loop dynamics are specified by the linear equation

$$\begin{bmatrix} \delta x'' \\ \delta y'' \end{bmatrix} - 2\omega \begin{bmatrix} 0 & 1 \\ -1 & 0 \end{bmatrix} \begin{bmatrix} \delta x' \\ \delta y' \end{bmatrix} - \begin{bmatrix} V_{xx} & V_{xy} \\ V_{xy} & V_{yy} \end{bmatrix} \begin{bmatrix} \delta x \\ \delta y \end{bmatrix} = 0 \quad (\text{B3})$$

The characteristic equation for this system is

$$\lambda^4 + [4\omega^2 - V_{xx} - V_{yy}]\lambda^2 + V_{xx}V_{yy} - V_{xy}^2 = 0 \quad (\text{B4})$$

For a singly hyperbolic unstable system, we can assume, in general, that

$$V_{xx}V_{yy} - V_{xy}^2 < 0 \quad (\text{B5})$$

The hyperbolic characteristic exponents of the system are computed from

$$\sigma^2 = -\frac{1}{2}[4\omega^2 - V_{xx} - V_{yy}] + \frac{1}{2}\sqrt{(4\omega^2 - V_{xx} - V_{yy})^2 - 4(V_{xx}V_{yy} - V_{xy}^2)} \quad (\text{B6})$$

which is guaranteed to be positive if the inequality in Eq. (B5) holds. The corresponding eigenvectors will be of the form

$$\mathbf{u}_{\pm} = \frac{1}{\sqrt{1 + u_{\pm}^2}} \begin{bmatrix} 1 \\ u_{\pm} \end{bmatrix} \quad (\text{B7})$$

$$u_{\pm} = \frac{\sigma^2 - V_{xx}}{V_{xy} \pm 2\omega\sigma} \quad (\text{B8})$$

$$u_{\pm} = \frac{V_{xy} \mp 2\omega\sigma}{\sigma^2 - V_{yy}} \quad (\text{B9})$$

The control acceleration that is added to the left-hand side of Eq. (B3) [corresponding to Eq. (34)] is

$$\sigma^2 G \begin{bmatrix} \frac{1}{1+u_+^2} + \frac{1}{1+u_-^2} & \frac{u_+}{1+u_+^2} + \frac{u_-}{1+u_-^2} \\ \frac{u_+}{1+u_+^2} + \frac{u_-}{1+u_-^2} & \frac{u_+^2}{1+u_+^2} + \frac{u_-^2}{1+u_-^2} \end{bmatrix} \begin{bmatrix} \delta x \\ \delta y \end{bmatrix} \quad (\text{B10})$$

Reforming the characteristic equation for this case yields

$$\lambda^4 + [4\omega^2 - \tilde{V}_{xx} - \tilde{V}_{yy}]\lambda^2 + \tilde{V}_{xx}\tilde{V}_{yy} - \tilde{V}_{xy}^2 = 0 \quad (\text{B11})$$

where

$$\tilde{V}_{xx} = V_{xx} - \sigma^2 G \left[\frac{1}{1+u_+^2} + \frac{1}{1+u_-^2} \right] \quad (\text{B12})$$

$$\tilde{V}_{yy} = V_{yy} - \sigma^2 G \left[\frac{u_+^2}{1+u_+^2} + \frac{u_-^2}{1+u_-^2} \right] \quad (\text{B13})$$

$$\tilde{V}_{xy} = V_{xy} - \sigma^2 G \left[\frac{u_+}{1+u_+^2} + \frac{u_-}{1+u_-^2} \right] \quad (\text{B14})$$

For this system to be linearly stable, three conditions must be met:

$$[4\omega^2 - \tilde{V}_{xx} - \tilde{V}_{yy}] > 0 \quad (\text{B15})$$

$$\tilde{V}_{xx}\tilde{V}_{yy} - \tilde{V}_{xy}^2 > 0 \quad (\text{B16})$$

$$[4\omega^2 - \tilde{V}_{xx} - \tilde{V}_{yy}]^2 - 4[\tilde{V}_{xx}\tilde{V}_{yy} - \tilde{V}_{xy}^2] > 0 \quad (\text{B17})$$

We note that condition (B15) can be rewritten as

$$4\omega^2 - V_{xx} - V_{yy} + 2\sigma^2 G > 0 \quad (\text{B18})$$

which can be satisfied for large enough G . Next, expanding condition (B16) results in

$$\begin{aligned} & \sigma^4 G^2 (u_+ - u_-)^2 - \sigma^2 G \left[(1+u_-^2) \{u_+^2 V_{xx} + V_{yy} - 2u_+ V_{xy}\} \right. \\ & \quad \left. + (1+u_+^2) \{u_-^2 V_{xx} + V_{yy} - 2u_- V_{xy}\} \right] \\ & \quad + (1+u_+^2)(1+u_-^2)(V_{xx}V_{yy} - V_{xy}^2) > 0 \end{aligned} \quad (\text{B19})$$

Again, we see that G can be chosen large enough to guarantee stability, as long as $u_+ \neq u_-$. Finally, we note that condition (B17) can be rewritten as

$$8\omega^2 [2\omega^2 - (\tilde{V}_{xx} + \tilde{V}_{yy})] + (\tilde{V}_{xx} - \tilde{V}_{yy})^2 + 4\tilde{V}_{xy}^2 > 0 \quad (\text{B20})$$

which, on inspection, reduces to the sufficient condition

$$2\omega^2 - \tilde{V}_{xx} - \tilde{V}_{yy} > 0 \quad (\text{B21})$$

or, equivalently,

$$2\omega^2 - V_{xx} - V_{yy} + 2\sigma^2 G > 0 \quad (\text{B22})$$

for which G can always be chosen large enough to stabilize. Should this condition be true, then condition (B18) follows trivially. Thus, we note that our proposed control law can always stabilize the hyperbolic unstable equilibrium point for large enough G . The attractiveness of this controller is that it has a natural specification for our time-varying system at each moment of time and depends only on the estimate of relative position between the spacecraft and an estimate of the position of the spacecraft on the nominal periodic orbit.

Note, if only the unstable manifold is nulled in the preceding control, the stability condition for large gain reduces to

$$2u_+ V_{xy} - u_+^2 V_{xx} - V_{yy} > 0 \quad (\text{B23})$$

where the assumption $V_{xx}V_{yy} - V_{xy}^2 < 0$ still holds. This condition is not necessarily satisfied and can be true or false depending on the values of the partials, meaning that control along the unstable manifold is not always sufficient. Thus, the stable manifold must also be nulled in this system if the resulting control is to stabilize all local motion for large enough values of gain. This can also be understood in the context of Hamiltonian systems. Assume we apply a control that maintains the basic Hamiltonian structure of our problem and that removes the unstable component of motion, but does not remove the exponentially stable component of motion. Then, due to the Hamiltonian structure of our system, there must be an associated exponential unstable component of the motion. Thus, any such control must remove both stable and unstable components of motion.

Acknowledgments

The work described here was funded in part by the NASA Office of Space Science and by the Interplanetary Network Technology Program by a grant from the Jet Propulsion Laboratory, California Institute of Technology, which is under contract with NASA. The authors appreciate the helpful comments of an anonymous referee and the Associate Editor.

References

- ¹Nemytskii, V. V., and Stepanov, V. V., *Qualitative Theory of Differential Equations*, Dover, New York, 1989, p. 152.
- ²Dunham, D. W., and Roberts, C. E., "Stationkeeping Techniques for Libration-Point Satellites," *Journal of the Astronautical Sciences*, Vol. 49, No. 1, 2001, pp. 127–144.
- ³Gómez, G., Masdemont, J., and Simo, C., "Quasihalo Orbits Associated with Libration Points," *Journal of the Astronautical Sciences*, Vol. 46, No. 2, 1998, pp. 135–176.
- ⁴Barden, B. T., and Howell, K. C., "Fundamental Motions Near Collinear Libration Points and Their Transitions," *Journal of the Astronautical Sciences*, Vol. 46, No. 4, 1998, pp. 361–378.
- ⁵Gómez, G., and Mondelo, J. M., "The Dynamics Around the Collinear Equilibrium Points of the RTBP," *Physica D*, Vol. 157, No. 4, 2001, pp. 283–321.
- ⁶DeCou, A. B., "Orbital Station-Keeping for Multiple Spacecraft Interferometry," *Journal of the Astronautical Sciences*, Vol. 39, No. 3, 1991, pp. 283–297.
- ⁷Gómez, G., Lo, M., Masdemont, J., and Museth, K., "Simulation of Formation Flight Near Lagrange Points for the TPF Mission," American Astronautical Society, AAS Paper 01-305, Aug. 2001.
- ⁸Schaub, H., Vadali, S. R., Junkins, J. L., and Alfriend, K. T., "Spacecraft Formation Flying Control Using Mean Orbit Elements," *Journal of the Astronautical Sciences*, Vol. 48, No. 1, 2000, pp. 69–87.
- ⁹Alfriend, K. T., and Schaub, H., "Dynamic and Control of Spacecraft Formations: Challenges and Some Solutions," *Journal of the Astronautical Sciences*, Vol. 48, Nos. 2–3, 2000, pp. 249–267.
- ¹⁰Koon, W. S., Marsden, J. E., Murray, R. M., and Masdemont, J., "J₂ Dynamics and Formation Flight," AIAA Paper 2001-4090, Aug. 2001.
- ¹¹Arnold, V. I., *Dynamical Systems III, Encyclopaedia of Mathematical Sciences*, Vol. 3, Springer-Verlag, Berlin, 1980, pp. 72, 73.
- ¹²Brouwer, D., and Clemence, G. M., *Methods of Celestial Mechanics*, Academic Press, New York, 1961, pp. 336–338.
- ¹³Howell, K. C., Barden, B. T., and Lo, M. W., "Application of Dynamical Systems Theory to Trajectory Design for a Libration Point Mission," *Journal of the Astronautical Sciences*, Vol. 45, No. 2, 1997, pp. 161–178.
- ¹⁴Scheeres, D. J., "Satellite Dynamics About Asteroids: Computing Poincaré Maps for the General Case," *Hamiltonian Systems with Three or More Degrees of Freedom*, edited by C. Simó, NATO Advanced Science Inst. Series, Vol. 533, Kluwer Academic, Norwell, MA, 1999, pp. 554–557.
- ¹⁵Howell, K. C., "Families of Orbits in the Vicinity of the Collinear Libration Points," *Journal of the Astronautical Sciences*, Vol. 49, No. 1, 2001, pp. 107–125.
- ¹⁶Cesari, L., *Asymptotic Behavior and Stability Problems in Ordinary Differential Equations*, 2nd ed., Academic Press, New York, 1963, pp. 55–59.
- ¹⁷Hsiao, F. Y., and Scheeres, D. J., "The Dynamics of Formation Flight About a Stable Trajectory," American Astronautical Society, AAS Paper 02-189, Jan. 2002.
- ¹⁸Marchal, C., *The Three-Body Problem*, Elsevier, New York, 1990, pp. 213–216.
- ¹⁹Scheeres, D. J., Han, D., and Hou, Y., "The Influence of Unstable Manifolds on Orbit Uncertainty," *Journal of Guidance, Control, and Dynamics*, Vol. 24, No. 3, 1999, pp. 573–585.
- ²⁰Dickson, L. E., *Elementary Theory of Equations*, Wiley, New York, 1914, p. 34.